JOC The Journal of Organic Chemistry

pubs.acs.org/joc Article

Assembly and Disassembly of Supramolecular Hypervalent Iodine Macrocycles via Anion Coordination

Krishna Pandey, Samsul Arafin, Eli Jones, Yachu Du, Gajanan C. Kulkarni, Ain Uddin, Toby J. Woods, and Kyle N. Plunkett*

Cite This: J. Org. Chem. 2024, 89, 7437−7445 Read Online

ACCESS | Metrics & More | Article Recommendations | Supporting Information

ABSTRACT: This study explores the dynamic self-assembly and disassembly of hypervalent iodine-based macrocycles (HIMs) guided by secondary bonding interactions. The reversible disassembly and reassembly of HIMs are facilitated through anion binding via the addition of tetrabutylammonium (TBA) salts or removal of the anion by the addition of silver nitrate. The association constants for HIM monomers with TBA(Cl) and TBA(Br) are calculated and show a correlation with the strength of the iodine−anion bond. A unique tetracoordinate hypervalent iodine-based compound was identified as the disassembled monomer. Last, the study reveals the dynamic bonding nature of these macrocycles in solution, allowing for rearrangement and participation in dynamic bonding chemistry.

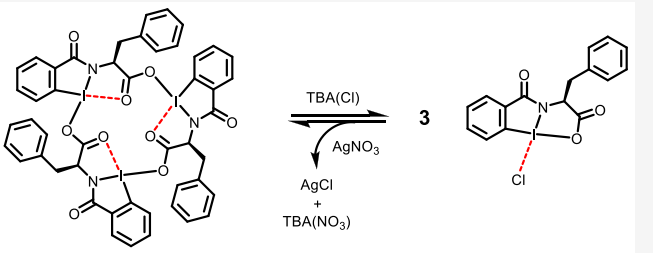

INTRODUCTION

The complex self-assembly of molecular building blocks is often facilitated by noncovalent interactions. Among these, hydrogen bonding, $\pi-\pi$ stacking, and van der Waals interactions are among the most commonly employed in constructing higher order structures within synthetic chemistry and structural biology. Rather than using these traditional noncovalent interactions, we are focused on preparing functional materials based on secondary noncovalent interactions involving hypervalent iodine. "Hypervalency" is a term given to elements in groups 15−18 of the periodic table bearing more electrons than an octet in their valence shell.[1] Of the many hypervalent-capable atoms (S, P, etc.), hypervalent iodine-based reagents have been the most systematically investigated over the past several decades owing to their structural diversity, reaction versatility, and position as an environmentally sustainable alternative to heavy-metal catalysts.[2,3] Secondary bonding is characterized as those interactions that involve intermolecular hypervalent connections with lengths shorter than the sum of the van der Waals radii between a heavy p-block element and an electron pair donor (typically O, N, S, or halogen).[4] Hypervalent iodine species are found as λ^3 or λ^5 arrangements at the oxidized iodine center. The λ^3 systems exhibit a "T" like binding motif where the two most electronegative atoms are most energetically favorable[5] when oppositely aligned linearly from the iodine to create a three-center four-electron (3c−4e) bond system,[6−8] where the bond length of one heteroatom with the iodine is dictated by the other heteroatom.[9] In addition, secondary bonding can arise in these systems from neighboring atom lone pairs. These added secondary bonding interactions can lead to insoluble materials if the interactions lead to uncontrolled long-range associations.[10,11] However, with proper design, such as intramolecular binding motifs, controlled assembly in these systems is possible.[12−14]

An early example of a hypervalent iodine-based macrocycle (HIM) that assembled by secondary bonding was demonstrated by Ochiai through the assembly of 1-alkynyl benziodoxolones in the solid state (Figure 1).[15] More recently, Tykwinski and Zhdankin described the preparation of HIMs based on amino-acid-functionalized benziodazoles (Figure 1).[16] The authors proposed that an initial preassembly of three oxidized benziodazoles (**5a−c**) through secondary bonding interactions (Scheme 1) allowed the rearrangement of the primary and secondary bonding to give stable macrocycles **6a−c** (e.g., proper linear alignment of the heteroatoms) that was stable both in the solid state as well as in solution. The energy of formation of the trimer was calculated to be 77 kcal/mol,[17] considerably greater than those found by Ochiai. Owing to the nature of the amino acid building blocks, these HIMs were chiral with functional groups exclusively occupying one face of the macrocycle. Other HIMs have also been developed based on benziodoxaboroles.[18]

Received: December 11, 2023
Revised: April 15, 2024
Accepted: April 29, 2024
Published: May 14, 2024

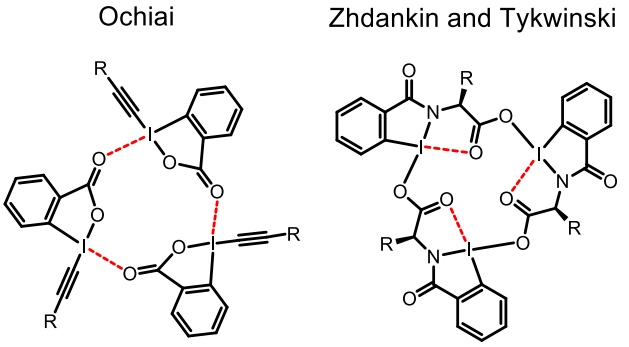

Figure 1. Hypervalent iodine-based macrocycles. Secondary bonding is represented by red dashes.

In this work, we were interested in probing the dynamic nature of the HIM assemblies in solution by investigating methods to assemble and disassemble the supramolecular structures through chemical means. Through heterogeneous macrocycle mixing, we demonstrate the macrocycles' participation in dynamic chemical bonding whereby the monomers are free to mix with neighboring macrocycles. Furthermore, we have investigated the association of a series of tetraalkylammonium salts, where anions compete for binding at the iodine center, leading to the complete disassembly of the macrocycles. Reassembly of the HIMs from these dissociated complexes is possible through abstraction of the halogen by silver nitrate, demonstrating the unique reversibility of this system.

RESULTS AND DISCUSSION

We prepared three HIM analogues based on those previously prepared with glycine and valine[16] in addition to a new phenylalanine derivative (Scheme 1). The HIM precursors were prepared via amidation of 2-iodobenzoic acid **1** with the respective *t*-butoxy-(**2a,b**) or methoxy-protected amino acids **2c** followed by deprotection. Commercially available starting peptides H-Val-O*t*Bu·HCl (**2a**), H-Phe-O*t*Bu·HCl (**2b**), and H-Gly-OMe·HCl (**2c**) coupled to give intermediate **3a**, **3b**, and **3c**, respectively. Intermediates **3a-c** were hydrolyzed to HIM precursors **4a-c**. Synthesis of the HIM was accomplished by the oxidation of intermediates **4a−c**. While dimethyldioxirane[19] was previously used for this step,[16] we found 3-chloroperbenzoic acid (*m*CPBA) to be just as effective and easier to use.

Nuclear magnetic resonance spectroscopy and mass spectrometry were used to confirm the formation of the HIMs.[16] In addition, previously unknown Phe-HIM **6b** was confirmed by single-crystal X-ray crystallography. Through multiple crystallography experiments, we found that Phe-HIM **6b** could be isolated as two solvomorphs (Figure 2). Crystals prepared through vapor diffusion of diethyl ether into chloroform yielded structures with (solvomorph I) or without (solvomorph II) a single chloroform solvent molecule

Scheme 1. Synthesis of Amino Acid-Based Hypervalent Iodine Macrocycle[a]

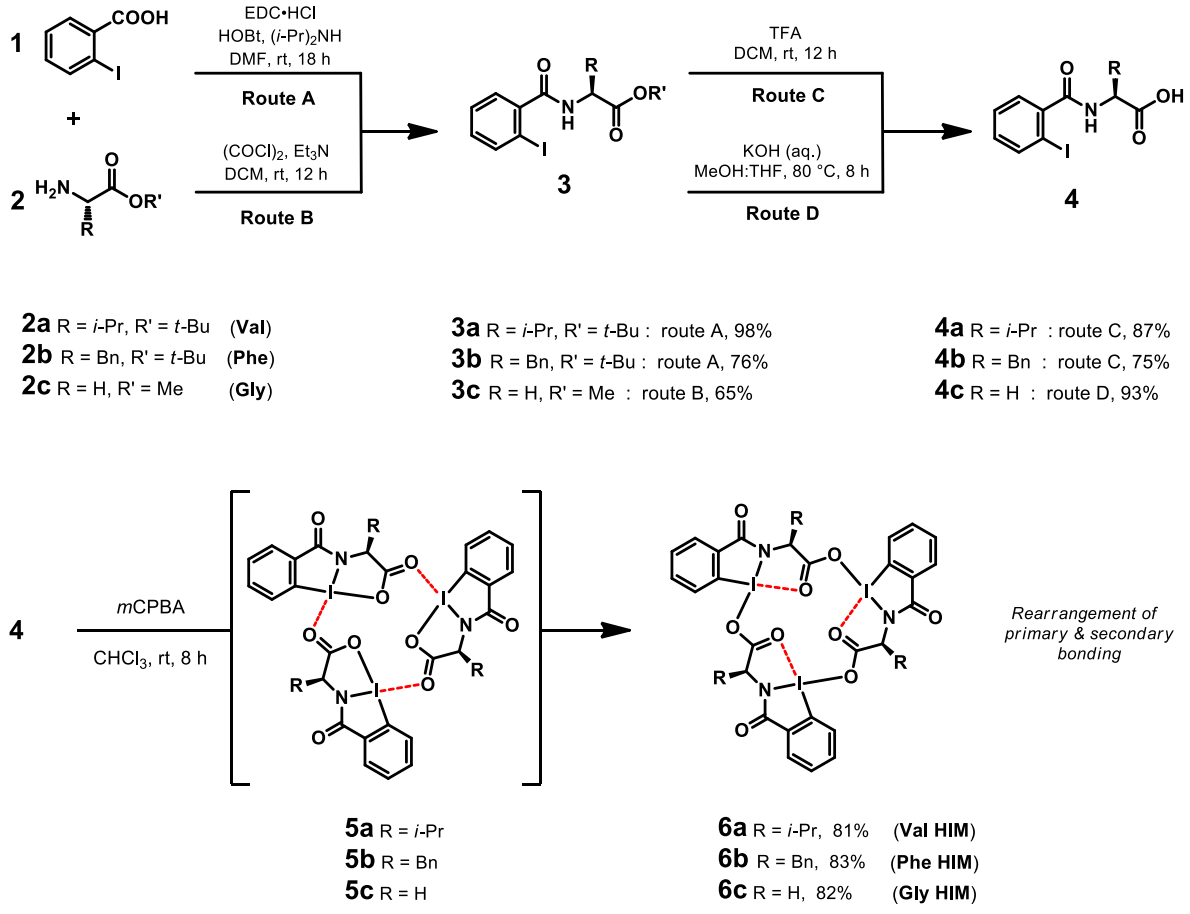

[a]Rearrangement of secondary bonding gives the more stable "T" binding motif around hypervalent iodine, leading to a stabilized macrocycle.

https://doi.org/10.1021/acs.joc.3c02830
J. Org. Chem. 2024, 89, 7437−7445

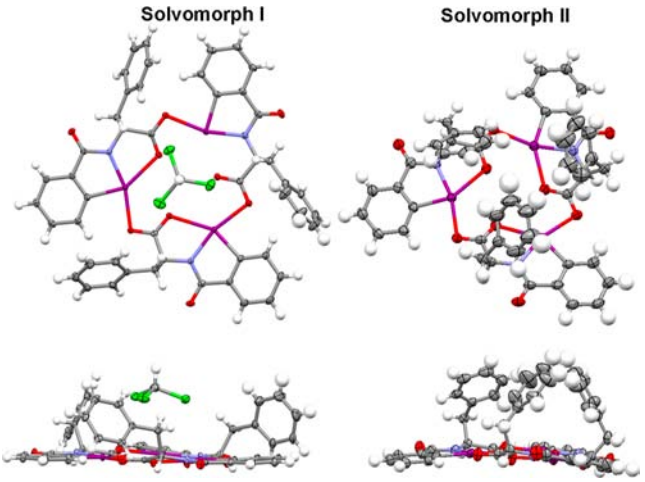

Figure 2. Solvomorphs I and II of Phe-HIM **6b**. A single chloroform molecule inclusion (solvomorph I) leads to the projection of benzyl groups away from the core, while crystals found from different experiments without chloroform inclusion (solvomorph II) project benzyl groups to a vertical arrangement. These models show a "bond" for the secondary bonding that is >2.5 Å (e.g., dotted line in the chemical structure in Scheme 1). Thermal ellipsoids are drawn at 50% probability.

incorporated into the lattice in separate crystallization experiments. While both solvomorphs were created from similar conditions, the difference in the resulting crystal structure could arise from a difference in the nucleation event that could arise from variation in concentration between experiments. The presence of chloroform in the crystal lattice (solvomorph I) led to sandwich-like complexes around a centrally located chloroform molecule (Supporting Information for dimeric representation, Figure SI4) where the benzyl groups were splayed toward the exterior of the macrocycle. Alternatively, in crystals without chloroform inclusion (solvomorph II), the benzyl groups were projected in a more vertical arrangement. Two variations of the molecular conformation were found with either three benzyls projected upward (Figure 2) or two benzyls projected upward (Figure SI5). While we do not pursue the topic in this article, the chiral alignment of the benzyl rings on a single side of the macrocycle suggests the possibility of dynamic host−guest chemistry with chiral aromatic species.

To better understand the thermal stability of the HIM-based functional materials, we investigated the HIM decomposition in solution and solid state. Solutions of Val-HIM **6a** in deuterated benzene were held at increasing temperatures and monitored over time. We found the HIMs to be stable for extended periods at temperatures below 70 °C with some decomposition observed at temperatures above this (Supporting Information, Figure SI1). Thermogravimetric analysis (TGA) of Val-HIM **6a** showed a weight loss initiated at 150 °C at a ramp of 10 °C/min. However, we found that the materials decomposed at lower temperatures if held for longer periods of time. We used differential scanning calorimetry (DSC) to hold samples of Val-HIM **6a** at isothermal conditions of 60, 80, and 100 °C (Supporting Information, Figure SI2). Decomposition was observed after 30 min at 100 °C, but the HIM was stable for hours at lower temperatures. The discrepancy between the TGA and DSC decomposition temperatures likely originates from the fast temperature ramp in TGA. We hypothesize that the prolonged elevated temperature at 100 °C drove off residual water/solvent from the sample, thereby initiating decomposition.

As a preliminary evaluation of associative processes in these HIM systems, we explored anion binding. For this, we studied the binding of HIMs via NMR titration with a series of commercially available tetrabutylammonium (TBA) salts in deuterated chloroform (Figure 3). From preliminary NMR

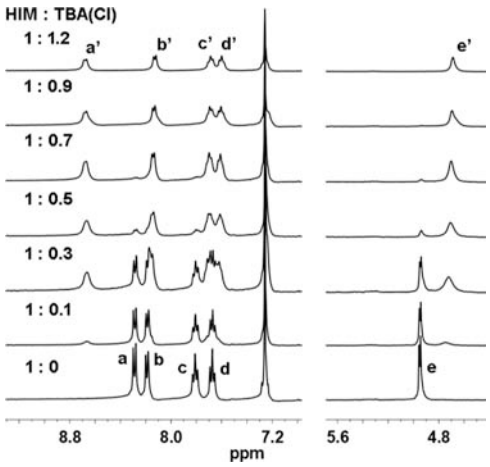

Figure 3. ^{1}H NMR titration of Val-HIM **6a** with TBA(Cl) at an incremental equivalency, starting from 0 to 1.2 equiv of TBA(Cl) in $CDCl_3$. More titration points are found in the Supporting Information (Figures SI10−SI17. Proton NMR signal designations similar to Phe HIM scaffold given in Figure 4.

titrations of Val-HIM **6a** with TBA(Cl), it was evident that a new complex or species was being formed in the presence of TBA(Cl). Figure 3 shows a titration of Val-HIM **6a** with increasing amounts of TBA(Cl) (additional data points can be found in the Supporting Information, Figure SI10). It is evident that aromatic protons (a−d) of Val-HIM **6a** convert into a new species (a′−d′) with the protons associated with **6a** being absent from the spectra by approximately 0.9 equiv of TBA(Cl). A similar trend was found for Phe-HIM **6b**. The structure of the new adduct was identified by X-ray crystallography of crystals grown from Phe-HIM **6b** and six equivalent of tetraethylammonium chloride [TEA(Cl)] (Figure 4). The new compound prepared was identified as monomeric species **7b** with an additional chloride ion associated with the electrophilic iodine center. While there are known hypervalent iodine organic compounds with I−Cl bonds,[20−23] these are all found as the λ^3 species. A similarity search of the Cambridge Crystallographic Data Center did not return any organic compounds with the four-coordinate binding motifs of **7b**. However, there are similarities to the known crystal structure of I_2Cl_6, the isolated dimer of ICl_3 that gives flat species with two chlorine atoms at distances of ∼2.38 Å and two chlorine atoms at distances of ∼2.70 Å.[24] The chloride is associated with the iodine in a secondary bonding environment. We believe this anion association is dynamic in solution, and the association and dissociation of chloride between other monomers is on the time scale of the NMR experiment, and therefore we see the average association in the NMR spectra. Through a series of crystallization experiments with all three HIM structures **6a−c**, we serendipitously isolated an intermediate disassembled structure of Gly-HIM **6c** where a single I−Cl bond is formed, but two benziodazoles remain bound together (Figure 5). Crystals of **8** were grown from the

https://doi.org/10.1021/acs.joc.3c02830
J. Org. Chem. 2024, 89, 7437−7445

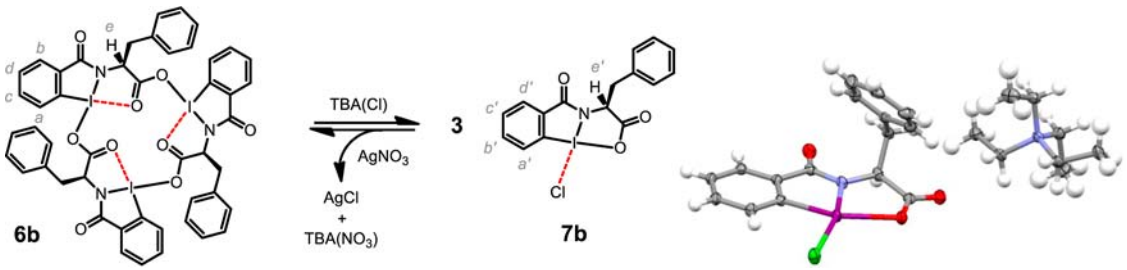

Figure 4. (Left) Scheme of Phe-HIM **6b** disassembly by addition of chloride anion. The HIM can reform when $AgNO_3$ is added to coordinate the chloride anion. (Right) Crystal structure of **7b** grown from TEA(Cl) showing the I−Cl bond that disrupts the secondary bonding self-assembly in the macrocycle. The I−Cl bond length is 2.707 Å, which is more typical of secondary bond lengths in hypervalent iodine centers. Thermal ellipsoids drawn at 50% probability.

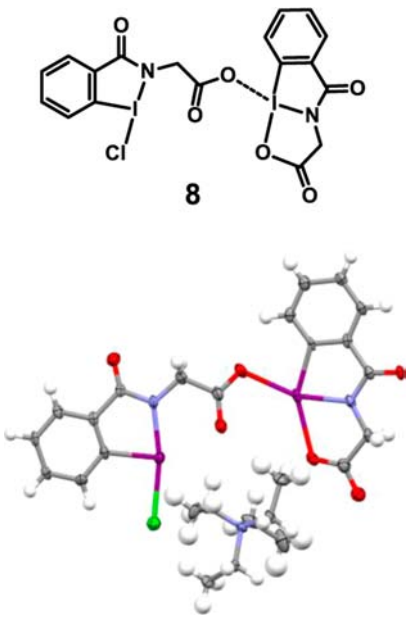

Figure 5. Crystal structure of a dimeric Gly-based benziodazole **8** with a single I−Cl bond. Crystal formed by slow diffusion of ethyl ether into a chloroform solution of **6c** with tetraethylammonium−chloride. Thermal ellipsoids drawn at 50% probability.

vapor diffusion technique by dissolving **6c** and tetraethylammonium-chloride (6 equiv) in a tube in chloroform and then placing in a chamber filled with diethyl ether. Further characterization of this compound was not possible owing to the lability of the structure. This structure suggests that a single chloride ion disrupts secondary bonding in the structure, causing disassembly of the HIM. With this information, we propose that the monomer, dimer, and trimer are in dynamic equilibrium, with the monomer most prevalent at low concentrations and the trimer most prevalent at high concentrations. The influence of chloride binding can be appreciated by looking at the changes in bond lengths around the iodine center for **6b**, **7b**, and **8** (Table 1, Supporting Information for bond length overlays, Figures SI6−SI8). The T-binding and three-center four-electron motif is most stable when the most electronegative species are in the trans configuration. HIM **6b** maintains bond lengths that preserve the T-bonding with an oxygen atom trans to the nitrogen atom (and a second oxygen in a secondary bonding arrangement). For the one iodine center bound to chlorine in dimer **8**, the chloride atom displaces an oxygen to adopt one of the trans positions and gives a relatively short I−Cl bond length of 2.553 Å. The oxygen is transferred into a secondary bonding role with a long I−O bond length of 2.683 Å. In the monomer **7b**, the oxygen readopts the trans position with an I−O bond of 2.444 Å, and the I−Cl bond lengthens to 2.707 Å. Of note, the second iodine center of **8** adopts a less common configuration where the bond length of the trans I−O bond (2.504 Å) is longer than the I−O bond (2.365 Å) that is typically assigned to a secondary bonding location. This is the reverse of typical bond lengths for these positions.

Table 1. Bond Lengths around Iodine Centers[a]

bond	**6b**[b]	**8** (I only)	**8** (I−Cl)	**7b**
I−O (short)	2.339(2)	2.364(9)		2.444(2)
I−C	2.101(3)	2.116(11)	2.126(11)	2.118(3)
I−N	2.105(3)	2.093(9)	2.148(11)	2.100(2)
I−O (long)	2.527(9)	2.504	2.683	
I−Cl			2.553(3)	2.707(7)

[a]Bond lengths in angstroms (Å). [b]Average bond lengths of the three iodine centers in the HIM.

Upon addition of enough TBA(Cl), monomeric species **7b** is the sole species in solution. To determine the nature of the I−Cl bond, we conducted a reversibility experiment by adding an excess of silver nitrate to the HIM/TBA(Cl) solution (Figure 4). We hypothesized that silver nitrate would abstract and precipitate as a bound chloride as AgCl, thereby allowing the benziodazoles to reassemble into the original HIM structures. Our observations confirmed this hypothesis, as the addition of silver nitrate to an NMR solution of **7b** followed by the removal of the precipitate produced an identical NMR spectrum compared to that of **6b** prior to the addition of the anion. With this observation, it provides an opportunity to reversibly form the assembled structure based on the presence of a chloride anion. It is important to note that other chloride-containing salts, such as NaCl, can also be used in the disassembly step. This is a unique type of dynamic equilibrium and could be used to build dynamic materials, something we are currently pursuing.

With our newly discovered knowledge of the reversible dissociation of the HIM structures and their resulting structures, we analyzed the ^{1}H NMR titrations to determine the association constant of the monomer−anion complex (H·G). For this, we prepared two primary solutions, one with a 12.9 mM concentration of HIM in $CDCl_3$ and a second stock solution (30−40×) of TBA salt. Incremental addition of the TBA stock solutions into each primary solution within an NMR tube enabled us to gradually raise the host-to-guest ratio while keeping the host concentration constant (12.9 mM). Although the host/guest (TBA salt) ratio can be determined

https://doi.org/10.1021/acs.joc.3c02830
J. Org. Chem. 2024, 89, 7437−7445

using accurate volumetric measurements, this approach is susceptible to error propagation. Instead, we relied on the integration of the eight α-amino protons of the TBA cation relative to the two reference protons from the monomer (fixed concentration). After establishing the H_0/G_0 ratio, we proceeded to determine the concentration of the H·G complex. To do this, we employed the same reference peak from the TBA analysis and integrated the adduct peak to determine the concentration.

With crystallographic proof of a 1:1 H·G complex, we fitted the titration data using a 1:1 model of monomer to salt (Figures 6 and SI3, SI10–SI17).[25,26] We achieved satisfactory

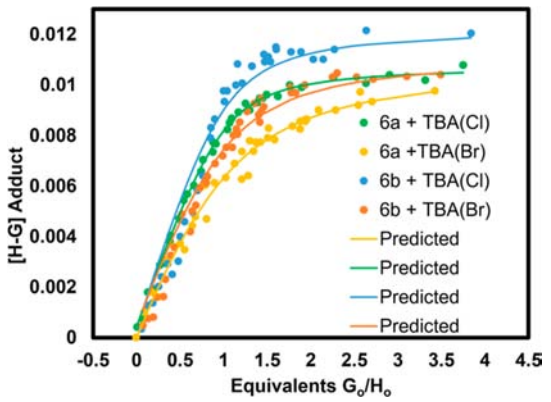

Figure 6. Isotherms of **6a** and **6b** titrated with TBA(Cl) or TBA(Br). The solid lines are the predicted model fits for each curve. $[H_0]$ is defined as the concentration of the benziodazole monomer (e.g., **3** benziodazole per HIM).

fits for the TBA(Cl) and TBA(Br) salts for both Val-HIM **6a** and the Phe-HIM **6b** systems. The calculated association constants for the monomer of Val-HIM **6a** with TBA(Cl) and TBA(Br) were 930 and 400 M^{-1}, respectively. The calculated association constants were reduced for the monomer of Phe-HIM **6b** with TBA(Cl) and TBA(Br) being 760 and 250 M^{-1}, respectively. Notably, the association constant magnitude correlated with the strength of the respective I–X bond, where X denotes the anion directly attached to the iodine. We also attempted to calculate association constants from titrations with TBA(F), TBA(OAc), and TBA(CN) but failed to derive meaningful association constants from this data owing to the steep curve slope. However, considering our interpretation of the direct correlation between the association constant and I–X bond strength, these results are justifiable. For large association constants, the precision of NMR titration makes it challenging to differentiate high-order association constants. Consequently, it is typically only conducted for binding constants below 1000 M^{-1} and suggests that these ions are binding with much higher affinities.[27] As an important control, NMR titrations with TBA(NO_3) showed no change in the HIM signals, demonstrating that the nitrate anion (or the TBA cation) does not interact with the hypervalent iodine. This was convenient as the byproduct for the HIM reassembly with $AgNO_3$ (Figure 4) is TBA(NO_3) and therefore does not interact with the reformed macrocycle. In addition, in the many crystallographic experiments between **6a** and **6b** with TBA(NO_3), only the HIM or salt was found as isolated crystals. Of note, TBA(I) was also evaluated, but the NMR solution turned a notable orange/yellow color and the spectra suggested decomposition in this system with molecular iodine most likely being formed under these conditions.

While NMR spectroscopy of the HIM species **6a–c** gives distinct and robust signals for the macrocycle, we were curious how dynamic the bonding in these systems was in the absence of additional anions. For example, once the macrocycle is formed, is it locked into its bonding arrangement or are the monomers free to rearrange with other macrocycles? To probe this question, we mixed solutions of Val-HIM **6a** with increasing amounts of Phe-HIM **6b** and probed the mixture with NMR spectroscopy. As shown in Figure 7, upon addition

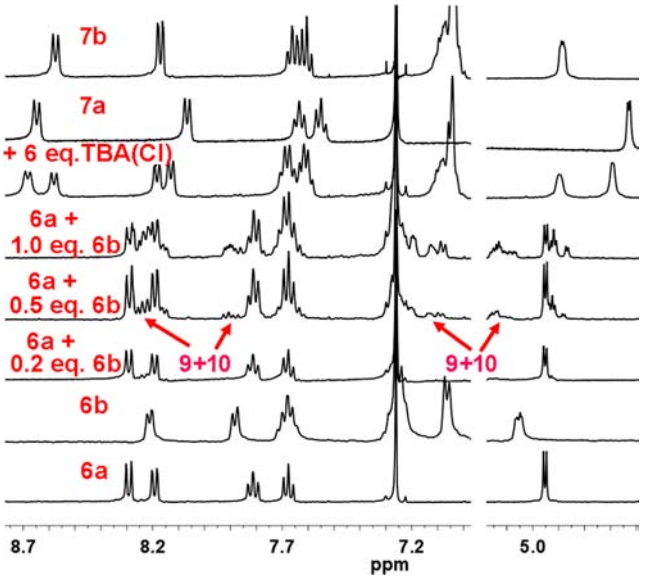

Figure 7. Scrambling experiment between Val-HIM **6a** with Phe-HIM **6b**. Mixed macrocycles **9** and **10** are formed as **6b** is added. Upon addition of TBA(Cl), the monomeric species **7a** and **7b** are formed, demonstrating that the new signals are not from decomposition. Slight shifting of the chemical shift of pure **7a** and **7b** with the mixture + TBA(Cl) is due to different concentrations of TBA(Cl) in the NMR experiments.

of 0.2 equiv of Phe-HIM **6b** we observed several distinct new peaks that were not present in either of the individual precursor HIM spectra. Upon the addition of a higher equivalence of Phe-HIM **6b** (1.0 equivalence), we found that the intensity of the new peaks increased. We propose that these are the result of macrocycles (e.g., **9** and **10**) with mixed compositions of the valine or phenylalanine side chains (Scheme 2). To demonstrate that the compounds are not decomposing, tetraethylammonium chloride (TEA(Cl)) was added to the mixture and resulted in clean NMR spectra of the I–Cl monomers **7a** and **7b**. This demonstrates that the monomers of the HIMs are free to rearrange their bonding in solution and provide a unique dynamic bonding character to the system. An initial version of this work was deposited in ChemRxiv on October 20, 2023.[29]

CONCLUSIONS

We have shown that the HIMs studied here provide a dynamic bonding system in which the structures can be easily disassembled and reassembled by the addition or removal of anions such as chloride, bromide, fluoride, and cyanide. In addition, the macrocycles are dynamic in solution even in the absence of additional anions and can exchange with other

https://doi.org/10.1021/acs.joc.3c02830
J. Org. Chem. 2024, 89, 7437–7445

Scheme 2. Probing the Dynamic Nature of the Secondary Bonding in HIMs[a]

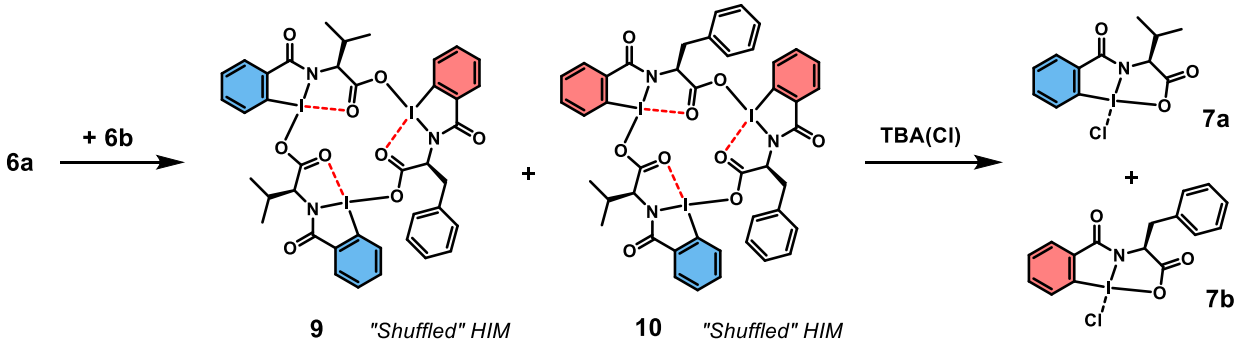

[a]Phe-HIM **6b** was added in substoichiometric amounts to **6a** and monitored via ^{1}H NMR (Figure 7). After scrambling was found, TBA(Cl) was added, and the I−Cl adducts **7a** and **7b** were obtained.

macrocycles to participate in dynamic covalent chemistry based on secondary bonding in these systems. Of note was the unique bonding around the hypervalent iodine center in the isolated monomers (e.g., **7b**). We plan to use the dynamic nature of these HIMs to build new materials that employ this reversibility.

EXPERIMENTAL SECTION

Unless otherwise noted, all reagents were used as received, and all reactions were carried out under an argon atmosphere. NMR spectra were recorded on a Varian 400 MHz NMR station at room temperature, unless otherwise noted.

2-(2-Iodo-benzoylamino)-3-methyl-butyric Acid *tert*-Butyl Ester (3a). To a 100 mL round-bottom flask were added 2-iodobenzoic acid (499 mg, 2.01 mmol) and 2 M oxalyl chloride (1.11 mL, 2.21 mmol) in 20 mL of extra dry CH_2Cl_2. A single drop of DMF was added to the solution. The reaction mixture was stirred at room temperature for 6 h. After removing the solvent excess oxalyl chloride under reduced pressure, the residue was dissolved in 25 mL of redistilled CH_2Cl_2 and added dropwise to a 100 mL ice-cooled round-bottom flask containing 10 mL of redistilled CH_2Cl_2, Et_3N (0.836 mL, 6.03 mmol), and L-valine *tert*-butyl ester hydrochloride (443 mg, 2.11 mmol). The mixture was stirred for 8 h at room temperature. CH_2Cl_2 (100 mL) was added to the solution to dissolve the suspended solid. The solution was washed with 1 N HCl (50 mL) twice to remove the extra amine, and then 50 mL of sat. $NaHCO_3$, followed by 50 mL water. The organic layer was dried with $MgSO_4$. The solvent was removed in vacuo. The residue was purified with column chromatography (hexane/ethyl acetate, 4/1) to afford 830 mg (98%) of 2-(2-iodo-benzoylamino)-3-methyl-butyric acid *tert*-butyl ester as a white solid. mp 73−75 °C; ^{1}H NMR (400 MHz, $CDCl_3$): δ 7.88 (d, J = 7.9 Hz, 1H), 7.43 (dd, J = 7.6, 1.8 Hz, 1H), 7.38 (td, J = 7.5, 1.0 Hz, 1H), 7.15−7.07 (m, 1H), 6.31 (d, J = 8.7 Hz, 1H), 4.65 (dd, J = 8.7, 4.4 Hz, 1H), 2.31 (dq, J = 11.4, 6.9 Hz, 1H), 1.51 (d, J = 10.0 Hz, 9H), 1.08 (d, J = 6.9 Hz, 3H), and 1.00 (d, J = 6.9 Hz, 3H). ^{13}C{^{1}H} NMR (100 MHz, $CDCl_3$): δ 170.8, 169.0, 142.1, 140.1, 131.3, 128.4, 128.2, 92.5, 82.4, 58.0, 31.8, 28.2, 19.2, and 18.0. Matched previous report.[16]

2-(2-Iodo-benzoylamino)-3-methyl-butyric Acid (4a). To a 100 mL round-bottom flask were added 2-(2-iodo-benzoylamino)-3-methyl-butyric acid (2.41 g, 6.0 mmol) and 50 mL of dry dichloromethane. After the system was cooled to 0 °C, TFA (15.0 g, 131 mmol) was added dropwise. The reaction mixture was warmed slowly to room temperature and stirred for 12 h. Excess TFA was removed by coevaporation with DCM and hexane three times, and the product was dried under high vacuum to obtain 1.80 g (87%) of pure white solid. mp 135−137 °C; ^{1}H NMR (400 MHz, $CDCl_3$): δ 7.89 (d, J = 8.0 Hz, 1H), 7.45−7.41 (m, 1H), 7.39 (d, J = 6.7 Hz, 1H), 6.30 (d, J = 8.4 Hz, 1H), 4.81 (dd, J = 8.6, 4.6 Hz, 1H), 2.55−2.15 (m, 1H), 1.13 (d, J = 6.9 Hz, 3H), and 1.05 (d, J = 6.9 Hz, 3H). ^{13}C{^{1}H} NMR (400 MHz, $CDCl_3$): δ 175.9, 169.8, 141.5, 140.1, 131.6, 128.6, 128.3, 92.4, 57.7, 31.4, 19.3, and 18.0. Matched previous report.[16]

Valine HIM (6a). 2-(2-Iodo-benzoylamino)-3-methyl-butyric acid (86 mg, 0.25 mmol) and 77% mCPBA (130 mg, 0.75 mmol) were dissolved in 6 mL of chloroform in a 10 mL round-bottom flask. The reaction was kept stirring at room temperature for 8 h. The reaction mixture was concentrated under vacuum at room temperature. The residue was suspended in 5 mL of diethyl ether followed by sonication. The precipitate formed was filtered and washed with 2 × 5 mL of diethyl ether to give 70 mg (81%) of the product as a white solid. mp 134−136 °C; ^{1}H NMR (400 MHz, $CDCl_3$): δ 8.27 (d, J = 8.1 Hz, 1H), 8.17 (d, J = 7.6 Hz, 1H), 7.78 (t, J = 8.3 Hz, 1H), 7.65 (t, J = 7.4 Hz, 1H), 4.92 (d, J = 4.5 Hz, 1H), 2.55 (td, J = 13.7, 6.8 Hz, 1H), 1.22 (d, J = 6.9 Hz, 3H), and 1.07 (d, J = 6.9 Hz, 3H). ^{13}C{^{1}H} NMR (400 MHz, $CDCl_3$): δ 178.9, 167.2, 134.6, 133.3, 130.9, 130.5, 130.1, 119.7, 63.6, 32.8, 20.3, and 17.7. Matched previous report.[16]

2-(2-Iodo-benzoylamino)-3-phenyl-propionic Acid *tert*-Butyl Ester (3b). To a solution of 2-iodo benzoic acid (1.0 g, 4.03 mmol) dissolved in 30 mL of DMF was added EDC.HCl (0.85 g, 4.4 mmol) and HOBt (0.68 g, 4.4 mmol) at 0 °C. The reaction mixture was sonicated to make the solution homogeneous, and argon bubbled through the solution for 15 min. L-phenylalanine *tert*-butyl ester hydrochloride (1.14 g, 4.4 mmol) was added, followed by diisopropylamine (1.35 g, 13.3 mmol). The mixture was stirred overnight, allowing the ice to melt and warm to room temperature. After the completion of the reaction, the solution was poured into 50 mL of water and extracted with ethyl acetate (3 × 25 mL). The organic layer was combined and washed with water (3 × 50 mL). Finally, the reaction mixture was washed with 50 mL of brine. The organic solution was dried with sodium sulfate and then concentrated to give an oil. The crude oil was purified using column chromatography with 20% ethyl acetate in hexane to yield 1.39 g (76%) of a white solid. mp 76−79 °C; ^{1}H NMR (400 MHz, $CDCl_3$): δ 7.86 (d, J = 7.8 Hz, 1H), 7.37−7.27 (m, 4H), 7.26−7.21 (m, 2H), 7.12−7.06 (m, 1H), 6.32 (d, J = 7.5 Hz, 1H), 4.95 (dt, J = 7.6, 6.0 Hz, 1H), 3.31−3.19 (m, 2H), and 1.43 (s, 9H). ^{13}C{^{1}H} NMR (400 MHz, $CDCl_3$): δ 170.3, 168.5, 141.4, 140.1, 136.1, 131.3, 129.7, 128.5, 128.2, 128.1, 127.0, 92.5, 82.7, 54.1, 38.0, and 28.0. HRMS (TOF MS ES+) m/z: $[M + Na]^+$ calcd for $C_{20}H_{22}INO_3Na$, 474.0542; found, 474.0549.

2-(2-Iodo-benzoylamino)-3-phenyl-propionic Acid (4b). To a 50 mL round-bottom flask were added 2-(2-iodo-benzoylamino)-3-phenyl-propionic acid *tert*-butyl ester (1.38 g, 3.07 mmol) and 30 mL of dry dichloromethane. After the system was cooled to 0 °C, TFA (8.8 g, 77 mmol) was added dropwise. The reaction was warmed slowly to room temperature and stirred for 12 h. Excess TFA was removed by coevaporation with DCM and hexane three times, and the product was dried under high vacuum to obtain 0.9150 g (75%) of pure white solid. mp 156−157 °C; ^{1}H NMR (400 MHz, DMSO-d_6):

https://doi.org/10.1021/acs.joc.3c02830
J. Org. Chem. 2024, 89, 7437−7445

δ 8.72 (d, J = 8.4 Hz, 1H), 7.85 (d, J = 7.1 Hz, 1H), 7.42 (t, J = 7.5 Hz, 1H), 7.30 (m, 4H), 7.23 (m, 1H), 7.18−7.10 (m, 2H), 4.69−4.44 (m, 1H), 3.17 (dd, J = 14.0, 4.7 Hz, 1H), and 2.97 (dd, J = 13.8, 10.3 Hz, 1H). $^{13}C\{^1H\}$ NMR (400 MHz, $CDCl_3$): δ 175.5, 169.4, 141.0, 140.3, 135.6, 131.7, 129.7, 128.9, 128.6, 128.3, 127.5, 92.5, 53.7, and 37.4. $^{13}C\{^1H\}$ NMR (400 MHz, DMSO-d_6): δ 172.9, 168.5, 142.2, 139.3, 137.9, 130.9, 129.2, 128.2, 127.9, 126.4, 93.3, 53.8, and 36.4. HRMS (TOF MS ES+) *m/z*: $[M + H]^+$ calcd for $C_{16}H_{15}INO_3$, 396.0097; found, 396.0096.

Phenylalanine HIM (6b). 2-(2-Iodo-benzoylamino)-3-phenyl-propionic acid (100 mg, 0.25 mmol) and 77% mCPBA (130 mg, 0.75 mmol) were dissolved in 10 mL of chloroform in a round-bottom flask. The reaction was kept stirring at room temperature for 8 h. The reaction mixture was concentrated by vacuum at room temperature. The residue was suspended in 10 mL of diethyl ether followed by sonication. The precipitate formed was filtered and washed with 2 × 5 mL of diethyl ether to give 82 mg (83%) of the product as a white solid. mp 135−136 °C; ^1H NMR (400 MHz, $CDCl_3$): δ 8.21 (dd, J = 7.3, 1.8 Hz, 1H), 7.90−7.84 (m, 1H), 7.74−7.60 (m, 2H), 7.31−7.26 (m, 1H), 7.23 (d, J = 6.9 Hz, 2H), 7.06 (d, J = 6.7 Hz, 2H), 5.05 (dd, J = 7.7, 3.1 Hz, 1H), 3.54−3.47 (m, 1H), and 3.42 (dd, J = 13.3, 7.6 Hz, 1H). $^{13}C\{^1H\}$ NMR (400 MHz, $CDCl_3$): δ 178.4, 167.1, 136.2, 134.3, 132.8, 130.5, 130.3, 130.1, 129.7, 128.3, 126.7, 120.6, 58.5, and 37.9. HRMS (TOF MS ES+) *m/z*: $[M + H]^+$ calcd for $C_{48}H_{37}I_3N_3O_9$, 1179.9664; found, 1179.9669.

(2-Iodo-benzoylamino)-acetic Acid Methyl Ester (3c). To a 100 mL round-bottom flask were added 2-iodobenzoic acid (499 mg, 2.01 mmol) and 2 M oxalyl chloride (1.11 mL, 2.21 mmol) in 20 mL of extra dry CH_2Cl_2. A single drop of DMF was added to the solution. The reaction mixture was stirred at room temperature for 6 h. After removing the solvent and the remaining oxalyl chloride under reduced pressure, the residue was dissolved in 25 mL of redistilled CH_2Cl_2 and added dropwise to a 100 mL ice-cooled round-bottom flask containing 10 mL of redistilled CH_2Cl_2, Et_3N (0.836 mL, 6.03 mmol), and glycine methyl ester hydrochloride (265 mg, 2.11 mmol). The mixture was stirred for 8 h at room temperature. CH_2Cl_2 (100 mL) was added to the solution to dissolve the suspended solid. The solution was washed with 1 N HCl (50 mL) twice to remove the extra amine, and then sat. $NaHCO_3$ (50 mL), followed by water (50 mL). The organic layer was dried with $MgSO_4$. The solvent was removed in vacuo. The residue was purified with column chromatography (hexane/acetone, 4/1) to afford 415 mg (65%) of (2-iodo-benzoylamino)-acetic acid methyl ester as a white solid. Melting point 97−99 °C; ^1H NMR (400 MHz, $CDCl_3$): δ 7.89 (d, J = 8.0 Hz, 1H), 7.45 (dd, J = 7.6, 1.8 Hz, 1H), 7.39 (t, J = 7.5 Hz, 1H), 7.12 (td, J = 7.6, 1.8 Hz, 1H), 6.33 (s, 1H), 4.26 (d, J = 5.0 Hz, 2H), and 3.81 (s, 3H). $^{13}C\{^1H\}$ NMR (400 MHz, $CDCl_3$): δ 170.1, 169.2, 141.3, 140.0, 131.4, 128.4, 128.2, 92.4, 52.5, and 41.7. HRMS (TOF MS ES+) *m/z*: $[M + H]^+$ calcd for $C_{10}H_{11}INO_3$, 319.9784; found, 319.9785. Previously reported.[28]

(2-Iodo-benzoylamino)-acetic Acid (4c). To a solution of (2-iodo-benzoylamino)-acetic acid methyl ester (134 mg, 0.42 mmol) in 2 mL of THF and 5 mL of methanol was added KOH (0.19 g, 3.5 mmol in 1.75 mL water). The reaction mixture was refluxed at 80 °C for 10 h in an oil bath. After the completion of the reaction, the solvent was evaporated under vacuum. Water (40 mL) was added to the residue, and then the reaction mixture was acidified with 1 N HCl to pH 1−2. The obtained precipitate was collected by filtration and washed with water. The precipitate was dried in vacuo to obtain 119 mg (93%) of a white solid of (2-iodo-benzoylamino)-acetic acid. Melting point 178−180 °C; ^1H NMR (400 MHz, DMSO-d_6): δ 12.63 (s, 1H), 8.69 (t, J = 5.9 Hz, 1H), 7.89 (dd, J = 7.9, 0.8 Hz, 1H), 7.46 (tt, J = 10.2, 5.1 Hz, 1H), 7.36 (dd, J = 7.6, 1.7 Hz, 1H), 7.28−7.12 (m, 1H), and 3.89 (d, J = 6.0 Hz, 2H). $^{13}C\{^1H\}$ NMR (400 MHz, DMSO): δ 171.0, 169.1, 142.2, 139.4, 131.1, 128.4, 128.0, 93.4, and 41.0. HRMS (TOF MS ES+) *m/z*: $[M + H]^+$ calcd for $C_9H_9INO_3$, 305.9627; found, 305.9629. Previously reported.[28]

Glycine HIM (6c). (2-Iodo-benzoylamino)-acetic acid (76 mg, 0.25 mmol) and 77% mCPBA (130 mg, 0.75 mmol) were dissolved in 6 mL of chloroform in a 10 mL round-bottom flask. The reaction was kept stirring at room temperature for 8 h. The reaction mixture was concentrated by vacuum at room temperature. The residue was suspended in 5 mL of diethyl ether followed by sonication. The precipitate formed was filtered and washed with 2 × 5 mL of diethyl ether to give 62 mg (82%) of the product as a white solid. mp 211−213 °C. The solid was insoluble in common solvents except after addition of salt (e.g., TBA-Cl) that disassembled the macrocycle. For further characterization, glycine HIM **6c** (5 mg, 0.0054 mmol) and TBA chloride (9 mg, 0.0324 mmol) were dissolved in 1 mL of chloroform in a vial. The partially dissolved glycine HIM **6c** was characterized by NMR and mass spectrometry. The carbon NMR could not be obtained due to the low solubility of the mixture. ^1H NMR (400 MHz, $CDCl_3$): δ 8.64 (d, J = 8.1 Hz, 1H), 8.09 (dd, J = 7.5, 1.4 Hz, 1H), 7.64 (t, J = 8.5 Hz, 1H), 7.56 (t, J = 7.4 Hz, 1H), and 4.23 (s, 2H). HRMS (TOF MS ES−) *m/z*: $[M]^-$ calcd for $C_9H_6NO_3ICl$ (monomeric species), 337.9081; found, 337.9076.

Valine HIM Adduct 7a. Valine HIM **6a** (5 mg, 0.0048 mmol) and TBA chloride (8 mg, 0.0288 mmol) was dissolved in 1 mL of chloroform in a vial. The mixture was set up for crystallization at room temperature through the vapor diffusion method using diethyl ether as a cosolvent. Within 48 h, crystals of **7a** (one TBA cation per monomeric species) were obtained and analyzed. ^1H NMR (400 MHz, $CDCl_3$): δ 8.64 (d, J = 7.9 Hz, 1H), 8.08 (d, J = 7.4 Hz, 1H), 7.66 (t, J = 7.6 Hz, 1H), 7.57 (t, J = 7.4 Hz, 1H), 4.66 (d, J = 1.3 Hz, 1H), 2.41−2.28 (m, 1H), and 1.09 (d, J = 6.9 Hz, 3H). (Note: one of the methyl group peaks is integrated with TBA peak at 0.94 ppm) $^{13}C\{^1H\}$ NMR (400 MHz, $CDCl_3$): δ 171.8, 164.9, 133.7, 133.1, 129.5, 129.1, 120.1, 62.7, 32.5, 19.8, and 17.8. HRMS (TOF MS ES−) *m/z*: $[M]^-$ calcd for $C_{12}H_{12}NO_3ICl$, 379.9550; found, 379.9548.

Phenylalanine HIM Adduct 7b. Phenylalanine HIM **6b** (5 mg, 0.0042 mmol) and tetraethylammonium chloride (4.2 mg, 0.0252 mmol) were dissolved in 1 mL of chloroform in a vial. The mixture was set up for crystallization at room temperature through the vapor diffusion method using diethyl ether as a cosolvent. Within 48 h, crystals of **7b** (one tetraethylammonium cation per monomeric species) were obtained and analyzed. ^1H NMR (400 MHz, $CDCl_3$): δ 8.55 (d, J = 7.2 Hz, 1H), 8.16 (dd, J = 7.5, 1.6 Hz, 1H), 7.64 (dtd, J = 22.9, 7.3, 1.3 Hz, 2H), 7.12−7.00 (m, 5H), 4.88 (dd, J = 4.7, 2.1 Hz, 1H), 3.66−3.48 (m, 1H), and 3.39−3.35 (m, 1H). $^{13}C\{^1H\}$ NMR (400 MHz, $CDCl_3$): δ 172.5, 165.3, 136.6, 133.5, 133.2, 129.8, 129.7, 129.3, 129.2, 127.8, 126.3, 120.1, 58.3, and 37.0. HRMS (TOF MS ES−) *m/z*: $[M]^-$ calcd for $C_{16}H_{12}NO_3ICl$, 427.9550; found, 427.9532.

■ ASSOCIATED CONTENT

Data Availability Statement

The data underlying this study are available in the published article and its Supporting Information.

Supporting Information

The Supporting Information is available free of charge at https://pubs.acs.org/doi/10.1021/acs.joc.3c02830.

Detailed experimental procedures, NMR spectra, and X-ray crystallography details (PDF)

Accession Codes

CCDC 2309218−2309222 contain the supplementary crystallographic data for this paper. These data can be obtained free of charge via www.ccdc.cam.ac.uk/data_request/cif, or by emailing data_request@ccdc.cam.ac.uk, or by contacting The Cambridge Crystallographic Data Centre, 12 Union Road, Cambridge CB2 1EZ, UK; fax: +44 1223 336033.

■ AUTHOR INFORMATION

Corresponding Author

Kyle N. Plunkett − *School of Chemical and Biomolecular Sciences, Southern Illinois University, Carbondale,*

https://doi.org/10.1021/acs.joc.3c02830
J. Org. Chem. 2024, 89, 7437−7445

Carbondale, Illinois 62901, United States; orcid.org/0000-0002-5691-7876; Email: kplunkett@chem.siu.edu

Authors

Krishna Pandey − *School of Chemical and Biomolecular Sciences, Southern Illinois University, Carbondale, Carbondale, Illinois 62901, United States*

Samsul Arafin − *School of Chemical and Biomolecular Sciences, Southern Illinois University, Carbondale, Carbondale, Illinois 62901, United States*

Eli Jones − *School of Chemical and Biomolecular Sciences, Southern Illinois University, Carbondale, Carbondale, Illinois 62901, United States*

Yachu Du − *School of Chemical and Biomolecular Sciences, Southern Illinois University, Carbondale, Carbondale, Illinois 62901, United States*

Gajanan C. Kulkarni − *School of Chemical and Biomolecular Sciences, Southern Illinois University, Carbondale, Carbondale, Illinois 62901, United States*

Ain Uddin − *School of Chemical and Biomolecular Sciences, Southern Illinois University, Carbondale, Carbondale, Illinois 62901, United States*

Toby J. Woods − *George L. Clark X-ray Facility and 3M Materials Laboratory, University of Illinois at Urbana−Champaign, Urbana, Illinois 61801, United States;* orcid.org/0000-0002-1737-811X

Complete contact information is available at: https://pubs.acs.org/10.1021/acs.joc.3c02830

Author Contributions

KP, SA, EJ, YD, GK, AU, and KNP contributed to synthetic aspects of the work. KP prepared crystals for X-ray analysis and performed the mixing studies. SA performed titration experiments and DSC. EJ performed titration experiments, performed isotherm analysis, and devised the reversibility experiment. TJW obtained and solved the X-ray structures. KNP envisioned the experimental direction of the project. The manuscript was written through contributions of all authors. All authors have given approval to the final version of the manuscript.

Notes

The authors declare no competing financial interest.

■ ACKNOWLEDGMENTS

We thank the National Science Foundation (#2003654) and the American Chemical Society Petroleum Research Fund (61467-ND1) for support of this work.

■ REFERENCES

(1) Musher, J. I. The Chemistry of Hypervalent Molecules. *Angew. Chem., Int. Ed.* **1969**, *8* (1), 54−68.

(2) Stang, P. J.; Zhdankin, V. V. Organic Polyvalent Iodine Compounds. *Chem. Rev.* **1996**, *96* (3), 1123−1178.

(3) Yoshimura, A.; Zhdankin, V. V. Advances in Synthetic Applications of Hypervalent Iodine Compounds. *Chem. Rev.* **2016**, *116* (5), 3328−3435.

(4) Alcock, N. W. Secondary Bonding to Nonmetallic Elements. In *Advances in Inorganic Chemistry and Radiochemistry*; Emeléus, H. J., Sharpe, A. G., Eds.; Academic Press, 1972; Vol. *15*, pp 1−58.

(5) Ochiai, M.; Sueda, T.; Miyamoto, K.; Kiprof, P.; Zhdankin, V. V. Trans Influences on Hypervalent Bonding of Aryl Λ3-Iodanes: Their Stabilities and Isodesmic Reactions of Benziodoxolones and Benziodazolones. *Angew. Chem., Int. Ed.* **2006**, *45* (48), 8203−8206.

(6) Rundle, R. E. Electron Deficient Compounds. II. Relative Energies of "Half-Bonds"'. *J. Chem. Phys.* **1949**, *17* (8), 671−675.

(7) Pimentel, G. C. The Bonding of Trihalide and Bifluoride Ions by the Molecular Orbital Method. *J. Chem. Phys.* **1951**, *19* (4), 446−448.

(8) Weinhold, F. A.; Landis, C. R. *Valency and Bonding*; Cambridge University Press, 2005; pp 275−306.

(9) Kiprof, P. The Nature of Iodine Oxygen Bonds in Hypervalent 10-I-3 Iodine Compounds. *Arkivoc* **2005**, *2005* (4), 19−25.

(10) Carmalt, C. J.; Crossley, J. G.; Knight, J. G.; Lightfoot, P.; Martín, A.; Muldowney, M. P.; Norman, N. C.; Orpen, A. G. An Examination of the Structures of Iodosylbenzene (PhIO) and the Related Imido Compound, PhINSO2−4-Me-C6H4, by X-Ray Powder Diffraction and EXAFS (Extended X-Ray Absorption Fine Structure) Spectroscopy. *J. Chem. Soc., Chem. Commun.* **1994**, No. 20, 2367−2368.

(11) Hiller, A.; Patt, J. T.; Steinbach, J. NMR Study on the Structure and Stability of 4-Substituted Aromatic Iodosyl Compounds. *Magn. Reson. Chem.* **2006**, *44* (10), 955−958.

(12) Macikenas, D.; Skrzypczak-Jankun, E.; Protasiewicz, J. D. A New Class of Iodonium Ylides Engineered as Soluble Primary Oxo and Nitrene Sources. *J. Am. Chem. Soc.* **1999**, *121* (30), 7164−7165.

(13) Macikenas, D.; Skrzypczak-Jankun, E.; Protasiewicz, J. D. Redirecting Secondary Bonds To Control Molecular and Crystal Properties of an Iodosyl- and an Iodylbenzene. *Angew. Chem., Int. Ed.* **2000**, *39* (11), 2007−2010.

(14) Zhdankin, V. V.; Protasiewicz, J. D. Development of New Hypervalent Iodine Reagents with Improved Properties and Reactivity by Redirecting Secondary Bonds at Iodine Center. *Coord. Chem. Rev.* **2014**, *275*, 54−62.

(15) Ochiai, M.; Masaki, Y.; Shiro, M. Synthesis and Structure of 1-Alkynyl-1,2-Benziodoxol-3(1H)-Ones. *J. Org. Chem.* **1991**, *56* (19), 5511−5513.

(16) Zhdankin, V. V.; Koposov, A. E.; Smart, J. T.; Tykwinski, R. R.; McDonald, R.; Morales-Izquierdo, A. Secondary Bonding-Directed Self-Assembly of Amino Acid Derived Benziodazoles: Synthesis and Structure of Novel Hypervalent Iodine Macrocycles. *J. Am. Chem. Soc.* **2001**, *123* (17), 4095−4096.

(17) Kiprof, P.; Zhdankin, V. Self-Assembly of Hypervalent Iodine through Primary and Secondary Bonding. *Arkivoc* **2003**, *2003*, 170−178.

(18) Nemykin, V. N.; Maskaev, A. V.; Geraskina, M. R.; Yusubov, M. S.; Zhdankin, V. V. Preparation and X-Ray Crystal Study of Benziodoxaborole Derivatives: New Hypervalent Iodine Heterocycles. *Inorg. Chem.* **2011**, *50* (21), 11263−11272.

(19) Taber, D. F.; DeMatteo, P. W.; Hassan, R. A. Simplified Preparation of Dimethyldioxirane (DMDO). *Org. Synth.* **2013**, *90*, 350.

(20) Willgerodt, C. Ueber Einige Aromatische Jodidchloride. *J. Prakt. Chem.* **1886**, *33* (1), 154−160.

(21) Keefer, R. M.; Andrews, L. J. A Study of the Proximity Effects of Substituents on the Dissociation of Iodobenzene Dichlorides. *J. Am. Chem. Soc.* **1959**, *81* (10), 2374−2379.

(22) Amey, R. L.; Martin, J. C. Synthesis and Reaction of Substituted Arylalkoxyiodinanes: Formation of Stable Bromoarylalkoxy and Aryldialkoxy Heterocyclic Derivatives of Tricoordinate Organoiodine-(III). *J. Org. Chem.* **1979**, *44* (11), 1779−1784.

(23) Kiyokawa, K.; Kosaka, T.; Kojima, T.; Minakata, S. Synthesis and Structure of Hypervalent Iodine(III) Reagents Containing Phthalimidate and Application to Oxidative Amination Reactions. *Angew. Chem., Int. Ed.* **2015**, *54* (46), 13719−13723.

(24) Boswijk, K. H.; Wiebenga, E. H. The Crystal Structure of I2Cl6(ICl3). *Acta Crystallogr.* **1954**, *7* (5), 417−423.

(25) Brynn Hibbert, D.; Thordarson, P. The Death of the Job Plot, Transparency, Open Science and Online Tools, Uncertainty Estimation Methods and Other Developments in Supramolecular Chemistry Data Analysis. *Chem. Commun.* **2016**, *52* (87), 12792−12805.

(26) http://supramolecular.org/, 2000.

(27) Fielding, L. Determination of Association Constants (Ka) from Solution NMR Data. *Tetrahedron* **2000**, *56* (34), 6151−6170.
(28) Marosvölgyi-Haskó, D.; Petz, A.; Takács, A.; Kollár, L. Synthesis of Tetrahydrophthalazine and Phthalamide (Phthalimide) Derivatives via Palladium-Catalysed Carbonylation of Iodoarenes. *Tetrahedron* **2011**, *67* (47), 9122−9128.
(29) Pandey, K.; Arafin, S.; Jones, E.; Du, Y.; Kulkarni, G.; Uddin, A.; Plunkett, K. N. Assembly and Disassembly of Supramolecular Hypervalent Iodine Macrocycles via Anion Coordination. *ChemRxiv* 2023. DOI: 10.26434/chemrxiv-2023-s7386.

NOTE ADDED AFTER ASAP PUBLICATION

This paper was published ASAP on May 14, 2024 with an incorrect TOC graphic. The corrected version was reposted on May 14, 2024.

https://doi.org/10.1021/acs.joc.3c02830
J. Org. Chem. 2024, 89, 7437−7445